This article has been accepted for publication in a future issue of this journal, but has not been fully edited. Content may change prior to final publication. Citation information: DOI 10.1109/JSEN.2018.2882736, IEEE Sensors Journal

Temperature Independent Defect Monitoring using Passive Wireless RFID Sensing System

Ali Imam Sunny, Jun Zhang, *Member, IEEE,* Gui Yun Tian, *Senior Member, IEEE,* Chaoqing Tang, Waqas Rafique, Aobo Zhao and Mengbao Fan

Abstract— **A significant requirement of low-cost sensing systems for defect detection is essential to bridge the gap of non-destructive testing & evaluation (NDT&E) and structural health monitoring (SHM). In practical situation, the temperature variation will be unknown in a priori and hence will give rise to uncertainty and unreliability in the defect detection. This paper demonstrates the potential use of low frequency (LF) RFID tag antenna based wireless sensors to characterise corrosion and crack progression in high-temperature conditions for potential structural monitoring. Consideration of the parasitic parameters which depend on the temperature variation is presented. The key factors that influences the sensing accuracy with regards to different materials due to inhomogeneity are presented. A cost-effective self-compensation method is proposed by means of a self-swept frequency measurement through selection and fusion of temperature dependent feature near the tag's resonance region. The experimental work validates the effectiveness of the method in temperature compensation and some initial results demonstrate the efficiency of the technique to overcome the inhomogeneity.**

***Index Terms*— Crack and corrosion detection, feature fusion, high temperature environment, passive radio frequency identification (RFID) sensors, self-swept-frequency compensation**

I. INTRODUCTION

Online monitoring of metallic structures at high temperature for defect detection is a key to many industrial NDT&E demands, such as power generation, oil and gas and nuclear industry [1, 2]. These industries do not allow connecting temperature sensitive integrated circuit (IC) to the measurement circuit or conditioning electronics using wired cables. With the development of sensors and the Internet of Things (IoT), defect detection and characterization techniques are enabled by embedding sensors for large-scale infrastructure. The ability to inspect defects or classify them without shutdown of industry for unscheduled time is an important economic consideration, and therefore, a monitoring method with temperature compensation ability is highly desirable. Many NDT&E methods can be used for high-temperature inspection and monitoring such as laser ultrasonic [3, 4], thermal infrared imaging technology [5] and laser electromagnetic acoustic transducer (EMAT) configurations [6-8]. However, these inspection techniques come with complexity and cost and for long-term measurements in condition monitoring applications. Temperature perturbations lead to changes in the physical and geometrical properties of the material causing changes in the measured signals due to thermal expansions and temperature induced changes in the sensors [9]. These variations are undesirable in NDT&E and SHM as they may be misinterpreted as being caused by defects. For real-life situations, two techniques have been applied to minimize errors caused by temperature fluctuations and these are; Optimal Baseline Selection (OBS) and Baseline Signal Stretch (BSS) [10-12]. OBS targets to select a best 'fit' from a baseline dataset which consists of signals from healthy structure at discrete temperatures. Once the best fit is identified, it is then used to determine damage detection. On the other hand, BSS aims to find the best 'correction' of a baseline recorded at different temperatures.

Several passive sensing systems are investigated to discern accurate temperature variation in harsh environments such as surface acoustic wave (SAW) sensors, wireless passive LC sensors, and thermocouples. High-temperature thermocouples can work in the temperature higher than 1000°C; however, this technique requires complex slip ring mechanisms to ensure electrical contact continuity due to weak output signal [13]. Previous studies have shown the use of SAW-RFID enabled temperature sensors performed well within 40°C [14] and later it was extended to 250°C [15]. Though a long readout distance can be obtained with SAW sensors because of absence of electronic devices, but they are easily influenced by the sound velocity which is strongly dependent on the temperature and other geometric properties. On the other hand, wireless passive LC sensors are suitable for temperature measurement in harsh environments, such as hermetic spaces [16] and rotating components [17].

The beneficial side of chip-less RFID is that it can operate in high temperature conditions [18]. However, in chip-less tags, the anti-collision techniques are totally dependent upon the reader, whereas in chip based tags, the IC is dedicated for tagging purposes.

The chipped passive wireless RFID sensors have gained much attention in both academies and industries for potential SHM [19, 20]. Low frequency (LF) and high frequency (HF) RFID sensors have been used previously to characterize the steel corrosion progression [21-24] and the read range was later improved by the usage of 3D ultra-high frequency (UHF) band RFID [25, 26]. However, communication and sensing in LF/HF RFID system is itself antithetical where the former is based on magnetic resonance coupling (MRC) and the latter relies on

Manuscript received October 9, 2018. This work was supported by the EPSRC Novel Sensing Networks for Intelligent Monitoring (NEWTON) project under Grant EP/J012343/1.

Ali Imam Sunny and Waqas Rafique are with the Department of Informatics, King's College London, WC2R 2LS, U.K. (email: ali.imam@kcl.ac.uk)

Jun Zhang is with the School of Information Engineering, Guangdong University of Technology, Guangzhou 510006, P. R. China. (email: junzhang@gdut.edu.cn)

Gui Yun Tian, Chaoqing Tang and Aobo Zhao are with the School of Engineering, Newcastle University, Newcastle upon Tyne, NE1 7RU, U.K. (email: g.y.tian@ncl.ac.uk)

Mengbao Fan is with the School of Mechanical Engineering, China University of Mining Technology, Xuzhou 221116, P. R. China. (email: wuzhi3495@cumt.edu.cn)

This article has been accepted for publication in a future issue of this journal, but has not been fully edited. Content may change prior to final publication. Citation information: DOI 10.1109/JSEN.2018.2882736, IEEE Sensors Journal

magnetic inductive coupling. Though time-domain based RFID system has immense communication speed over frequency domain [27], but the latter has advantageous in terms of working at different resonant frequencies. Most of the passive RFID sensors in the UHF band are based on tag's response information in frequency domain [28]. Temperature evaluation for LF RFID sensing system is still an area to be explored.

The aim of this paper is trying to use sweep frequency measurement to compensate for the temperature influence and therefore to improve the robustness of defect detection. This is done by understanding the physical behavior of the related parameters and the defect and temperature influence along with time-frequency feature extraction method in conjunction with feature selection and fusion to characterize defects.

II. Methods and Measurement Principles

The possible interferences of using RFID sensing system can be roughly categorized into three types: *system configurations* such as the communication distance and the circuit bandwidth, *sample interferences* such as roughness, geometry, thickness, permittivity and permeability and *operating conditions* such as temperature. In practical situations, the unknown temperature variation and defect will be mixed. This section presents the temperature modeling, test instrumentation, and feature extraction of LF RFID sensing system.

A. Sensing principles with varying temperature

Commercial RFID tags are designed for non-metallic environments. For NDT&E applications e.g. crack depth detection on metallic samples, the detuning of RFID tag's impedance at presence of nearby conductor needs be considered. The Bolch-Grüneisen formula mathematically represents the relationship between temperature and resistivity for metals [29] which shows that a impedances decreases with increasing temperature:

$$\rho(T) = \rho(0) + A(\frac{T}{\theta_R})^n \cdot \tag{1}$$

Where, $\rho(0)$ is the residual resistivity due to defect scattering. θ_R is the Debye temperature and A is constant. At high temperatures, the metal resistivity increases with an increase in temperature.

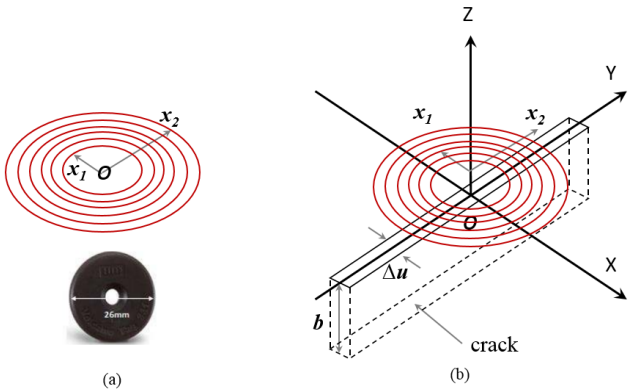

Fig. 1. Tag and specimen geometry. (a) LF RFID tag and spiral coil and (b) spiral coil with infinitely long crack in a conducting magnetic half-space.

The tag is modeled in Fig. 1. The coil is assumed to be planar spiral and air-cored with N turns, inner radius x_1, outer radius x_2, μ_0 is the permeability of free space. Therefore, the inductance of the spiral coil can be written in the form [30]:

$$L_0 = \frac{\mu_0 \pi N^2}{(x_2 - x_1)^2} \int_0^\infty \frac{1}{\alpha^4} I^2(\alpha x_1, \alpha x_2) d\alpha \,, \tag{2}$$

where I is the radial integral. The integral in Eq. (2) can be expressed in terms generalized functions. In addition, The crack is assumed to have constant depth b and width Δu. The results derived by Harfield and Bowler [31-33] can be used to derive the results for the tag's impedance.

In case of semiconductors, the fractional change in resistivity is negative which means that the resistivity of semi-conductor decreases exponentially with an increase in temperature [34]. Semiconductor components of an RFID tag, such as tag IC, also have a temperature dependence given by the Steinhart-Hart equation. The resistivity of semiconductor decreases with an increase in temperature and thus reducing the magnitude of the tag's response [29]:

$$\frac{1}{T} = A + B\ln(\rho) + C(\ln(\rho))^3 \cdot \tag{3}$$

Where, T is the temperature in degrees Kelvin and A, B, C are the coefficient constants that determines the expected resistance variation along with the temperature change. The electrical capacitance present in the RFID tag is a function of the dielectric constant of tag substrate. When the tag is exposed to change in temperature, there is a variation in the dielectric constant. This capacitance change in response to the temperature is expressed as:

$$C_T(T) = \frac{\varepsilon_0 \varepsilon_r(T) A}{t} \tag{4}$$

Where, ε_0 is the permittivity of free space and ε_r is the dielectric constant of the dielectric material which changes with temperature variation. A indicates the area of the electrode plate and t is the thickness of the dielectric material. Further, the eq. (2) can be expressed as [30]

$$L_T = n^2 \mu_0 R\left[\ln\left(\frac{8R}{a}\right) - 1.75\right] \tag{5}$$

Where, n is the coil turn, R is the loop radius, a is the wire radius.

B. Readout instrumentation for sweep frequency measurement

When the tag resonance oscillation occurs, the input impedance of the reader coil varies [35]. In order to measure the resonance frequency range, a readout circuit generates a swept-frequency signal in a specific frequency range is depicted in Fig. 2. The basic principle of LF RFID system is to discern variation of the tag with regards to the capacitance, resistance, inductance physical parameters by monitoring resonance frequency, input impedance, or Q-factor where each of the physical quantities are explained in detail [36]. The

differentiation method of these parameters can be represented as:

$$\Delta f_s = -\frac{1}{4\pi\left(L_R C_R\right)^{3/2}}\left[C_R,\ L_R,\ 0\right]\times\left[\Delta L_R,\ \Delta C_R,\ \Delta R_R\right]^{\mathrm{T}} \quad (6)$$

$$\Delta Q = \left[\frac{1}{2\left(R_s C_s\right)}\sqrt{C_s/L_s},\ -\frac{L_s}{2\left(R_s C_s^2\right)}\sqrt{C_s/L_s},\ -\frac{1}{2R_s^2}\sqrt{C_s/L_s}\right]\times\left[\Delta L_s,\ \Delta C_s,\ \Delta R_s\right]^{\mathrm{T}} \quad (7)$$

$$\Delta Z_x = \begin{bmatrix} 2\pi L_R k^2 Q,\ 2\pi L_R f_s k^2, \\ 4\pi L_R f_s k Q \end{bmatrix}\times\left[\Delta f_s,\ \Delta Q,\ \Delta k\right]^{\mathrm{T}}. \quad (8)$$

Where Δf_s is the resonant frequency which indicates the point when a variation appears in the frequency response of the impedance. ΔQ is the quality factor which is generally interpreted as an indication of the sharpness of the resonance. The higher the quality factor of the reader and the tag coils, the better the efficiency of the wireless power transfer (WPT) [37]. Z is the impedance, the subscript 'x' represents the resistive load either high or low i.e. the bit '1' or '0', and 'Δ' is the change caused by temperature or defect, and $k = M/\sqrt{L_R L_T}$ is the coupling coefficient.

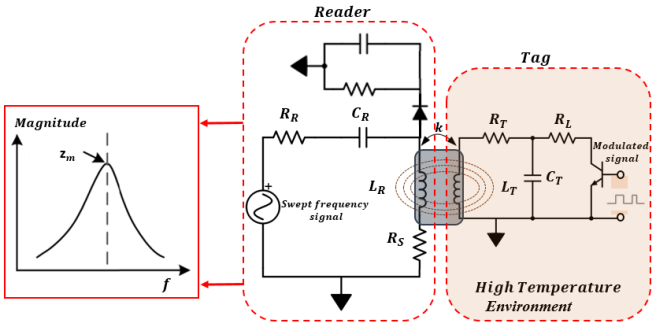

Fig. 2. Schematic of RFID sensing system.

The ambient temperature variation causes a change in the permittivity ε_r of the coil material following a change in the capacitance which results in the change of resonance frequency of the sensor. The change in this resonance frequency can be detected by the reader coil which is magnetically coupled with the tag. A sweep signal which covers the variation range of resonance frequency of the tag, is changed from the RFID reader, when the transmitted frequency equals the resonance frequency of the tag, resonance oscillation occurs and thus the input impedance of the reader coil changes [35].

C. *Feature extraction and selection*

The signal processing method is depicted in Fig. 3. The tag's resonance response can be obtained by changing the source frequency. From this, the impedance can be measured using *peak-to-peak* (P2P) response [22]. Then, the temperature coefficient across the swept frequency is compared, where the summation from both sides of the resonant frequency point is taken in order to enhance the robustness of the RFID sensing system. This new feature is presented as Fused P2P (FP2P). The sweep frequency technique gives the advantage of selecting various frequency ranges to extract information, the detailed behavior is going to be analyzed in the following section.

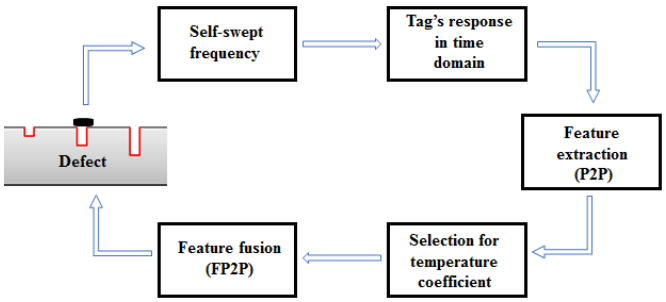

Fig. 3. Feature extraction processing diagram with a fusion based on combination of positive and negative temperature coefficients.

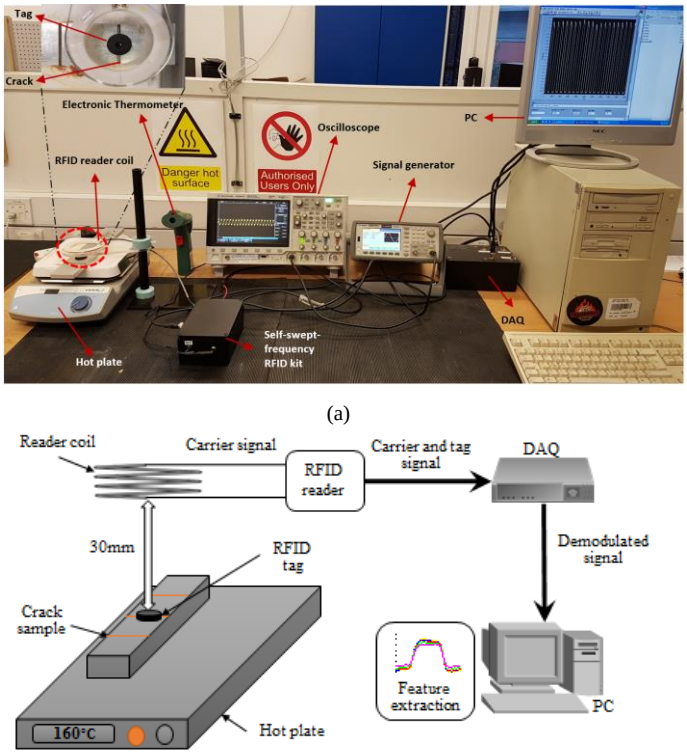

Fig. 4. Setup of RFID sensing system. (a) RFID system configuration and (b) schematic diagram with well-established reader and tag configuration.

III. Results and Discussions

A. *Experimental setup*

A LF RFID reader was used to perform the experimental work. The tag used is 231 Volcano LF RFID tag [38] as it was a suited tag to work in high temperature environment. The tag was programmed with an ID consisting of '1's' at a data bit rate of 125 kHz / 32 = 3.906 kHz with 50% duty cycles. Uniform stream of 1's was chosen for easier processing as it allows averaging over many cycles. The influence of distance variation was experimentally performed in [39] and based on this the optimum distance between the reader and the tag was found to

be 30 mm which has been used in this study. However, noteworthy to mention that at this setup the sample under the test's temperature does not affect the electronic property of the reader. The reader coil used was 90 mm in diameter with parameters of R = 10.45 Ω and L = 732 uH, and a quality factor of 32.25. Both the reader and the tag coils have a resonant frequency of 125 kHz in free space. Due to presence of a conductive material nearby the frequency band can shift. The signal from the reader coil was demodulated by the internal circuitry of the board in order to remove the carrier and obtain the envelope. The output signal of the demodulation circuit was sampled using a 14-bit Adlink 2010 DAQ at 1 MHz for 0.01 seconds (10,000 data points). The data acquisition was controlled in the PC using a LabVIEW program that allows the user to set the sample rate and number of samples to be acquired.

The experiment was carried out at five different temperatures which are 25ºC, 60ºC, 95ºC, 130ºC and 160ºC. The temperature was varied using a hot plate (VWR VHP-C7). These temperature increments were monitored using an electric thermometer. Fig. 4 shows the system setup and block diagram. When the swept carrier frequency was controlled by the Signal Generator, the tag's time domain response under a variation of carrier frequency was read out in the PC. This helps to measure the voltage change at a periodical frequency variation rather than at a certain frequency.

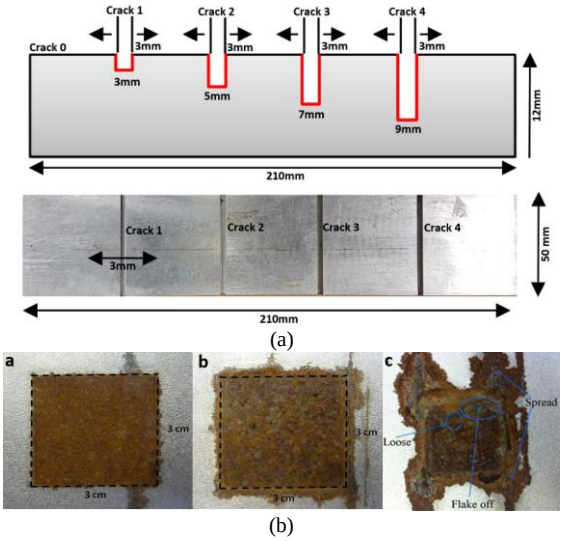

Fig. 5. (a) Aluminium sample with different crack depths. (b) Steel corrosion progression samples 1 month, 6 months and 10 months respectively.

Typical defects, on pipeline for example, are geometrical anomalies, metal loss and crack-like defects. The test involved an aluminium sample with an electrical conductivity of 25.8 MS/m and a geometrical dimension of 210 mm × 50 mm × 12 mm, which is shown in Fig. 5(a). This sample has machined slit defects of constant width of 3 mm. For reference convenience, these cracks are represented as C1 = 3 mm, C2 = 5 mm, C3 = 7 mm, C4 = 9 mm. And no crack which is 0 mm representing the healthy state is given as C0.

Also the corrosion progression samples are shown in Fig. 5(b) which indicates the spreading of corrosion over the time. Five corrosion progression samples have been used starting from no corrosion denoted as M0, corrosion progression in 1 month, 3 months, 6 months, 10 months and 12 months which are denoted as M1, M3, M6, M10 and M12 respectively. The measurements were repeated 10 times for each defect and the average value from those 10 measurements are then used as the measured result for further extraction.

B. Invariant feature fusion for crack depth characterization

The envelope of the RFID signal was captured with temperature increment from 25°C to 160°C. As the carrier frequency is swept, there is an increase in the tag's impedance once the excitation frequency matches the resonant frequency from the tag. The sweep frequency technique gives the flexibility to select various frequency ranges to extract robust information from it. Fig. 6 shows the tag's responses for varying temperature on plain metal. It can be observed that the temperature variation has a significant influence on the tag's performance which can be wirelessly captured by the reader. Because the quality factor of the reader coil is low, the overshoot in the step response casued by limit bandwidth of the reader coil is not apparent.

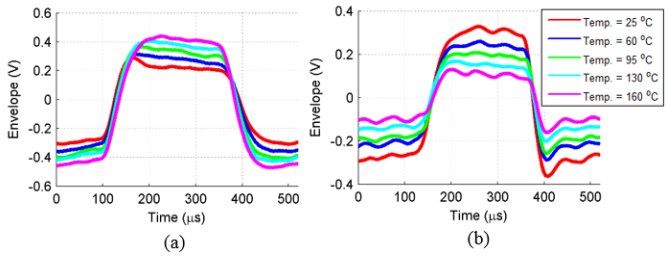

Fig. 6. Influence of temperature variation on the RFID signal. At (a) 130kHz and (b) 144kHz.

The time-frequency feature representations of P2P versus swept-frequency range for five temperature variations and five crack depths are displayed in Figs. 7(a-e). Comparing with the case in the air, it can be seen that the presence of the metallic sample leads to an approximate 14.0-kHz increase of the resonant frequency i.e. from 130 kHz to 144 kHz. It can be observed that the influence of the crack to the P2P response is higher than that of the temperature influence. This is because the growth of crack constantly improves the coupling coefficient between the reader and the tag coils or the magnetic flux penetrating into the tag coil, showing strong agreement with the sensing principle in Section 2. Also the increase of the distance between the reader and the tag has a negative influence in P2P but a negligible influence on the resonant frequency [39].

From Fig. 7 (a) at 25°C it can be seen that the maximum resonance of C4 is at 136 kHz whereas in (e) at 160°C the resonance have been shifted at lower than 132 kHz indicating a sensitivity of 0.03 kHz/°C. From Fig. 7 (b-d), the temperature is incremented at 35°C reaching up to 130°C and finally to 160°C respectively. Similarly, at a fixed temperature for example, in Fig. 7 (b) at 60°C, there is also a decrease in the

This article has been accepted for publication in a future issue of this journal, but has not been fully edited. Content may change prior to final publication. Citation information: DOI 10.1109/JSEN.2018.2882736, IEEE Sensors Journal

resonance frequency for all the cracks i.e. as the depth of the crack increases from 0 mm to 9 mm, the resonant frequency also shifts from approximately 138 kHz to approximately 134 kHz, indicating a sensitivity of 0.44 kHz/mm. Figs. 7 (a-e) show the shift in resonant frequency towards the lower frequency region with an increase in both temperature and crack depths but both the crack and the temperature are invariant in the higher frequency region. Next, P2P response in the steady state is used to characterise the crack progression from these frequency responses.

Fig. 8 (a) presents the RFID response for the temperature sensitivity along the crack depth at varying frequencies respectively and the temperature sensitivity is calculated by:

$$Temperature\ sensitivity = [P2P(160°C) - P2P(25°C)] \Big/ 135°C \quad (9)$$

At 133 kHz, a near zero temperature coefficient is obtained. At 139 kHz, because it is at resonant frequency, so with an increase in temperature the resistivity of semiconductor decreases and thus reducing the magnitude of the tag's response. However, the magnitude of the tag's response increases with an increase in crack depth due to higher coupling coefficient and an increased quality factor of the tag's coil. At 144 kHz, due to negative temperature coefficient, the P2P decreases with an increase in temperature and so does the magnitude of the crack depth decreases as well. Fig. 8 (b) depicts the resonant frequency response for both the crack progression and temperature increment and it can be observed for both the increments, the sensitivity decreases.

TABLE I
TEMPERATURE INDUCED UNCERTAINTY AT DIFFERENT FREQUENCY POINTS

Crack (mean ± error)	P2P at 130 kHz (V)	P2P at 133 kHz (V)	P2P at 139 kHz (V)	P2P at 144 kHz (V)	FP2P (V)
C0	0.293 ± 0.145	0.458 ± 0.126	0.536 ± 0.103	0.345 ± 0.141	0.638 ± 0.119
C1	0.496 ± 0.168	0.701 ± 0.046	0.731 ± 0.130	0.367 ± 0.190	0.863 ± 0.022
C2	0.743 ± 0.206	0.951 ± 0.034	0.884 ± 0.215	0.337 ± 0.205	1.079 ± 0.013
C3	0.998 ± 0.197	1.176 ± 0.060	1.000 ± 0.274	0.312 ± 0.210	1.311 ± 0.023
C4	1.273 ± 0.196	1.400 ± 0.082	1.060 ± 0.310	0.303 ± 0.218	1.577 ± 0.022

The temperature uncertainty for different frequency response and the fusion is shown in Table I. It is evident that both the mean response and the error is the maximum at 139 kHz. That is to say, the resonant frequency shows the maximum influence with the temperature variation. Whereas, near zero response with the lowest variation can be seen at 133 kHz. Therefore, this frequency can be selected in order to compensate for the temperature. In addition, by the summation of the positive temperature coefficient at 130 kHz and negative temperature coefficient at 144 kHz, we can obtain the lowest error in comparison to the rest and this fusion of feature enhances the robustness even in comparison to 133 kHz by approximate 3 times.

Fig. 9 shows the results of the time-frequency feature selection and fusion. The perk of using sweeping frequency is that, the response at near zero temperature coefficient could be observed which tends to give the lower temperature influence and thus giving robust crack characterization. From Fig. 9 (a) it can be observed that the crack progression is easily characterized using the near zero temperature coefficient i.e. 133 kHz. However, there is still a variation in the temperature and for this reason, feature fusion is carried out.

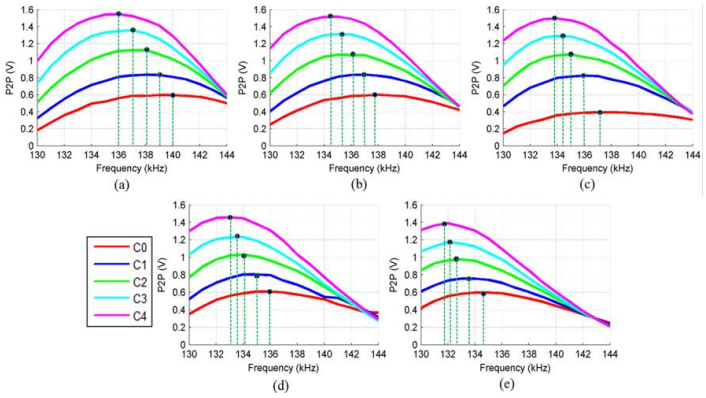

Fig. 7. Influence of temperature variation on P2P response of the RFID signal. At (a) 25°C, (b) 60°C, (c) 95°C, (d) 130°C, and (e) 160°C.

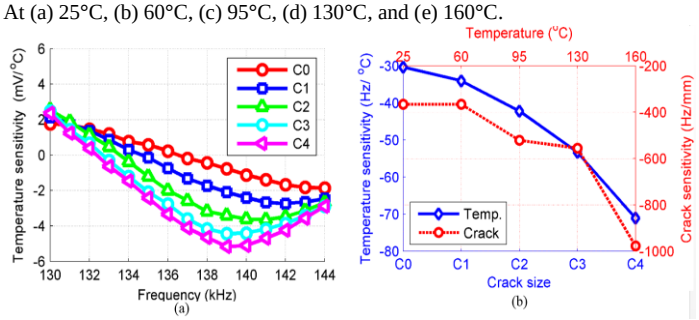

Fig. 8. Influence of temperature variation on P2P response of the RFID signal. (a) Showing temperature sensitivity under variation of frequency and (b) shows the respective temperature and crack sensitivities.

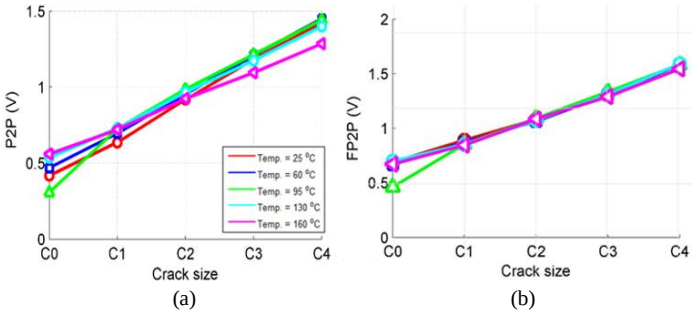

Fig. 9. Feature selection and extraction for crack characterization. At (a) near zero response with the lowest variation at 133 kHz and (b) temperature independent feature after feature fusion.

Fig. 9 (b) shows robust temperature independent feature based on a combination of positive and negative temperature coefficients near the resonance region. This is obtained by the

This article has been accepted for publication in a future issue of this journal, but has not been fully edited. Content may change prior to final publication. Citation information: DOI 10.1109/JSEN.2018.2882736, IEEE Sensors Journal

summation of peak-to-peak features in both single frequency points i.e. P2P at 130 kHz and P2P at 144 kHz. This means that the temperature influence can be suppressed by the addition of both the positive and negative coefficients. However, if only the single frequency is used for the feature extraction, the crack can somehow be detected but the effect of temperature and its influence will still persist. This may result in ineffective crack detection and characterization. Therefore, using a fused feature of FP2P, the temperature influence is removed while enhancing the sensitivity of LF RFID sensing system for robust NDT monitoring and robust crack progression monitoring.

C. Inhomogeneity case study using steel corrosion progression samples

Any variation in the distance between the RFID tag and the sample or any temperature variation, will change the impedance *Z*, inductance *L* and quality factor *Q* with coupling coefficient *k*. Following the equations above, the parameters *Z*, *L* and *Q* can be shown as:

$$Z, L \text{ or } Q = f(x, \rho, \mu) \tag{10}$$

Where x is the gap between the RFID tag and the sample, ρ is the resistivity of the sample and μ is the permeability of the sample [40]. Mainly ρ and μ of the measured sample highly influences the sensing coil. This influence causes measurement errors which is known as inhomogeneity (electrical run out). Inhomogeneity will disturb the propagation of the eddy currents and have an effect on the reader output such as noise and thereby degrade the resolution. The ρ and μ in steel corrosion samples are different to that of the aluminium crack samples. In this case study, the amplitude variation with resonant frequency shift for steel corrosion sample is considered and then the proposed feature fusion technique is implemented to reduce the effect of inhomogeneity.

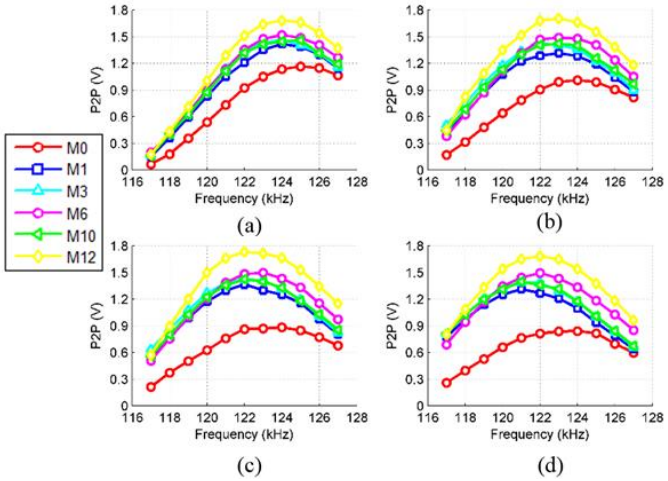

Fig. 10. Influence of temperature variation on P2P response for corrosion progression samples at (a) 25°C, (b) 60°C, (c) 95°C, and (d) 130°C.

Theoretically increasing the excitation/oscillating frequency can reduce the influence of the resistivity of the sample. The effect of inhomogeneity is monitored at different oscillating frequency for the corrosion progression samples. The measurement is taken from 118 kHz to 130 kHz with increments of 1 kHz. From Fig. 10, it is evident that the inhomogeneity in ferrous materials (steel) is higher than that of the non-ferrous materials (aluminium) as shown in Fig. 7. One of the main influences is due to the higher resistivity ρ and permeability μ in steel corrosion samples compared to aluminium sample.

The resonance frequency of the RFID tag can be seen to be shifted by about 10 kHz from aluminium to steel sample. Also it is abundantly clear, that the influence of conductivity is more than the amplitude change, thus to reduce the uncertainty in RFID measurements due to inhomogeneity, electrical conductivity must be mitigated. However, using our proposed fusion technique where the positive and the negative temperature coefficients are added together, these influences can be vanquished. Fig. 11 shows the corrosion progression characterization after feature fusion is applied.

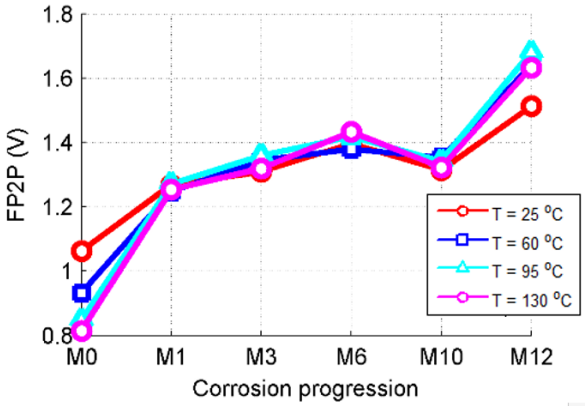

Fig. 11. Temperature independent corrosion progression characterization.

Over time, an increase in the corrosion thickness means an increase in the corrosion contribution to the RFID responses. This leads to a reduction of the electrical conductivity and permeability of the corroded region. Therefore, a monotonic trend with corrosion exposure time can be observed with an exception of sample M10 as this sample has been receded from its original state causing the measurement value to drop slightly.

IV. Conclusions and Future Work

In practical situation, the unknown temperature variation will give rise to uncertainty and unreliability, affecting the robustness in defect detection and characterization using LF RFID sensing system. A feature extraction and fusion method is proposed to address this problem. Through a sweep frequency measurement, positive and negative temperature coefficients in the left and right side of tag's resonant frequency are reported in this paper. This phenomena is used to compensate for the uncertainty caused by the temperature variation in both crack and corrosion characterization. However, due to the effect of inhomogeneity and the complex multi-layered structure of the corrosion samples, further quantification of magnetic permeability and electrical conductivity requires addressing. Feature fusion have been used

to suppress the temperature influence and effectively characterize corrosion but it is worth considering and exploring the RFID measurements in order that multiple parameter estimation can be achieved (corrosion progression and crack depth) with an extension to permeability and conductivity estimation as well. The robust LF RFID sensing system provides an alternative way for in-situ online monitoring of defects. This paper has demonstrated the possibility of bridging the gap between the NDT&E and SHM based on the passive LF RFID sensing system.

ACKNOWLEDGMENT

The authors would like to thank the International Paint LtD, Gaseshead, Newcastle, U.K. for providing the experimental samples and also EPSRC NEWTON project for funding the research work.

REFERENCES

[1] J. Li, J. Meng, X. Kang, Z. Long, and X. Huang, "Using Wireless Sensor Networks to Achieve Intelligent Monitoring for High-Temperature Gas-Cooled Reactor," *Science and Technology of Nuclear Installations,* vol. 2017.

[2] H. F. Rashvand and A. Abedi, *Wireless Sensor Systems for Extreme Environments: Space, Underwater, Underground and Industrial*: John Wiley & Sons, 2017.

[3] H. Nakano and S. Nagai, "Crack measurements by laser ultrasonic at high temperatures," *Japanese journal of applied physics,* vol. 32, p. 2540, 1993.

[4] A. McNab, K. J. Kirk, and A. Cochran, "Ultrasonic transducers for high temperature applications," *IEE Proceedings-Science, Measurement and Technology,* vol. 145, pp. 229-236, 1998.

[5] R. Usamentiaga, P. Venegas, J. Guerediaga, L. Vega, J. Molleda, and F. G. Bulnes, "Infrared thermography for temperature measurement and non-destructive testing," *Sensors,* vol. 14, pp. 12305-12348, 2014.

[6] X. Jian, I. Baillie, and S. Dixon, "Steel billet inspection using laser-EMAT system," *Journal of Physics D: Applied Physics,* vol. 40, p. 1501, 2007.

[7] A. Idris, C. Edwards, and S. B. Palmer, "Acoustic wave measurements at elevated temperature using a pulsed laser generator and an electromagnetic acoustic transducer detector," *Nondestructive Testing and Evaluation,* vol. 11, pp. 195-213, 1994.

[8] I. Baillie, P. Griffith, X. Jian, and S. Dixon, "Implementing an ultrasonic inspection system to find surface and internal defects in hot, moving steel using EMATs," *Insight-Non-Destructive Testing and Condition Monitoring,* vol. 49, pp. 87-92, 2007.

[9] Y. Yao, S. T. E. Tung, and B. Glisic, "Crack detection and characterization techniques—An overview," *Structural Control and Health Monitoring,* vol. 21, pp. 1387-1413, 2014.

[10] A. J. Croxford, P. D. Wilcox, B. W. Drinkwater, and G. Konstantinidis, "Strategies for guided-wave structural health monitoring," *Proceedings of the Royal Society of London A: Mathematical, Physical and Engineering Sciences,* vol. 463, pp. 2961-2981, Nov. 2007.

[11] Y. Lu and J. E. Michaels, "A methodology for structural health monitoring with diffuse ultrasonic waves in the presence of temperature variations," *Ultrasonics,* vol. 43, pp. 717-731, 2005.

[12] G. Konstantinidis, P. D. Wilcox, and B. W. Drinkwater, "An investigation into the temperature stability of a guided wave structural health monitoring system using permanently attached sensors," *IEEE Sensors Journal,* vol. 7, pp. 905-912, 2007.

[13] T. J. Bajzek, "Thermocouples: a sensor for measuring temperature," *IEEE Instrumentation & Measurement Magazine,* vol. 8, pp. 35-40, 2005.

[14] A. Kang, C. Zhang, X. Ji, T. Han, R. Li, and X. Li, "SAW-RFID enabled temperature sensor," *Sensors and Actuators A: Physical,* vol. 201, pp. 105-113, 2013.

[15] R. Fachberger and A. Erlacher, "Monitoring of the temperature inside a lining of a metallurgical vessel using a SAW temperature sensor," *Procedia Chemistry,* vol. 1, pp. 1239-1242, 2009.

[16] S. J. Prosser, "Advances in sensors for aerospace applications," *Sensors and Actuators A: Physical,* vol. 37, pp. 128-134, 1993.

[17] R. W. Johnson, J. L. Evans, P. Jacobsen, J. R. Thompson, and M. Christopher, "The changing automotive environment: high-temperature electronics," *IEEE Transactions on Electronics Packaging Manufacturing,* vol. 27, pp. 164-176, 2004.

[18] H. Cheng, X. Ren, S. Ebadi, Y. Chen, L. An, and X. Gong, "Wireless passive temperature sensors using integrated cylindrical resonator/antenna for harsh-environment applications," *IEEE Sensors Journal,* vol. 15, pp. 1453-1462, 2015.

[19] Z. Meng and Z. Li, "RFID Tag as a Sensor-A Review on the Innovative Designs and Applications," *Measurement Science Review,* vol. 16, pp. 305-315, 2016.

[20] J. Zhang, G. Y. Tian, A. M. J. Marindra, A. I. Sunny, and A. B. Zhao, "A review of passive RFID tag antenna-based sensors and systems for structural health monitoring applications," *Sensors,* vol. 17, p. 265, 2017.

[21] M. Alamin, G. Y. Tian, A. Andrews, and P. Jackson, "Corrosion detection using low-frequency RFID technology," *Insight-Non-Destructive Testing and Condition Monitoring,* vol. 54, pp. 72-75, 2012.

[22] A. I. Sunny, G. Y. Tian, J. Zhang, and M. Pal, "Low frequency (LF) RFID sensors and selective transient feature extraction for corrosion characterisation," *Sensors and Actuators A: Physical,* vol. 241, pp. 34-43, 2016.

[23] H. Zhang, R. Yang, Y. He, G. Y. Tian, L. Xu, and R. Wu, "Identification and characterisation of steel corrosion using passive high frequency RFID sensors," *Measurement,* vol. 92, pp. 421-427, 2016.

[24] A. I. Sunny and G. Y. Tian, "Enhanced sensitivity of low frequency (LF) RFID sensor signal for structural health monitoring (SHM) in high temperature environment," in *Proc. 9th World Conf. Non Destruct. Test.*, pp. 1-8, 2016.

[25] J. Zhang and G. Y. Tian, "UHF RFID tag antenna-based sensing for corrosion detection & characterization using principal component analysis," *IEEE Transactions on Antennas and Propagation,* vol. 64, pp. 4405-4414, 2016.

[26] A. Zhao, G. Y. Tian, and J. Zhang, "IQ signal based RFID sensors for defect detection and characterisation," *Sensors and Actuators A: Physical,* vol. 269, pp. 14-21, 2018.

[27] J. Vemagiri, A. Chamarti, M. Agarwal, and K. Varahramyan, "Transmission line delay - based radio frequency identification (RFID) tag," *Microwave and optical technology letters,* vol. 49, pp. 1900-1904, 2007.

[28] A. P. Sample, D. J. Yeager, P. S. Powledge, A. V. Mamishev, and J. R. Smith, "Design of an RFID-based battery-free programmable sensing platform," *IEEE Transactions on Instrumentation and Measurement,* vol. 57, pp. 2608-2615, 2008.

[29] A. Bid, A. Bora, and A. K. Raychaudhuri, "Temperature dependence of the resistance of metallic nanowires of diameter⩾ 15 nm: Applicability of Bloch-Grüneisen theorem," *Physical Review B,* vol. 74, p. 035426, 2006.

[30] R. J. Ditchburn, S. K. Burke, and M. Posada, "Eddy-current nondestructive inspection with thin spiral coils: Long cracks in steel," *Journal of Nondestructive Evaluation,* vol. 22, pp. 63-77, 2003.

[31] N. Harfield and J. R. Bowler, "Theory of thin-skin eddy-current interaction with surface cracks," *Journal of applied physics,* vol. 82, pp. 4590-4603, 1997.

[32] J. R. Bowler and N. Harfield, "Thin-skin eddy-current interaction with semielliptical and epicyclic cracks," *IEEE transactions on magnetics,* vol. 36, pp. 281-291, 2000.

[33] J. R. Bowler and N. Harfield, "Evaluation of probe impedance due to thin-skin eddy-current interaction with surface cracks," *IEEE Transactions on Magnetics,* vol. 34, pp. 515-523, 1998.

[34] D. K. Schroder, *Semiconductor material and device characterization*: John Wiley & Sons, 2006.

[35] K. G. Ong, C. A. Grimes, C. L. Robbins, and R. S. Singh, "Design and application of a wireless, passive, resonant-circuit environmental monitoring sensor," *Sensors and Actuators A: Physical,* vol. 93, pp. 33-43, 2001.

[36] Q.-A. Huang, L. Dong, and L.-F. Wang, "LC Passive Wireless Sensors Toward a Wireless Sensing Platform: Status, Prospects, and Challenges," *Journal of Microelectromechanical Systems,* vol. 25, pp. 822-841, 2016.

[37] S. Assawaworrarit, X. Yu, and S. Fan, "Robust wireless power transfer using a nonlinear parity–time-symmetric circuit," *Nature,* vol. 546, pp. 387-390, 2017.

[38] X. Ma, A. J. Peyton, and Y. Y. Zhao, "Eddy current measurements of electrical conductivity and magnetic permeability of porous metals," *NDT & E International,* vol. 39, pp. 562-568, 2006.

[39] J. Zhang, A. I. Sunny, G. Zhang, and G. Y. Tian, "Feature Extraction for Robust Crack Monitoring Using Passive Wireless RFID Antenna Sensors," *IEEE Sensors Journal,* vol. 18, pp. 6273-6380, 2018.

[40] G. Y. Tian, Z. X. Zhao, and R. W. Baines, "The research of inhomogeneity in eddy current sensors," *Sensors and Actuators A: physical,* vol. 69, pp. 148-151, 1998.